Electronic Supporting Information

Efficient near-infrared (NIR) polymer light-emitting diodes (PLEDs) based on heteroleptic Iridium(III) complexes with effect of intramolecular hydrogen bond or BF_2-chelation

Guorui Fu, Hao Zheng, Yani He, Wentao Li, Xingqiang Lü and Hongshan He

Materials and methods

Reagents and solvents were received from Sigma Aldrich and used without furtherpurification. All solvents, unless otherwise stated were degassed and stored over 3 Å activated molecule sieves prior to use. All manipulations of air and water sensitive compounds were carried out under dry N_2 using the standard Schlenk line techniques.

Elemental analyses were performed on a Perkin-Elmer 240C elemental analyzer. Fourier Transform Infrared (FT-IR) spectra were recorded on a Nicolet Nagna-IR 550 spectrophotometer in the region 4000-400 cm^{-1} using KBr pellets. ^1H NMR spectra were recorded on a JEOL EX 400 spectrometer with $SiMe_4$ as internal standard in $CDCl_3$ at room temperature. ^{19}F NMR spectrum was performed on a JEOL EX 100 spectrometer with $CFCl_3$ as internal standard in $CDCl_3$ at room temperature.ESI-MS was performed on a Finnigan LCQ^{DECA} XP HPLC-MS_n mass spectrometer with a mass to charge (*m/z*) range of 4000 using a standard electro-spray ion source and MeCN as the solvent. Electronic absorption spectra in the UV/Visible/NIR region were recorded with a Cary 300 UV spectrophotometer. Visible

emission and excitation spectra were collected by a combined fluorescence lifetime and steady-state spectrometer (FLS-980, Edinburgh) with a 450 W Xe lamp. Excited-state decay times were obtained by the same spectrometer but with a μF900 Xe lamp. The luminescent quantum yield (Φ_{em}) in solution was measured with free-base tetraphenylporphyrin (Φ_r = 0.13 in toluene solution at 298 K) as the standard.[1] The solution was degassed by three freeze-pump-thaw circles. The following equation was used to calculate quantum yields:

$$\Phi_s = \Phi_r \cdot [(n_s^2 \cdot A_r \cdot I_s)/(n_r^2 \cdot A_s \cdot I_r)]$$

Where Φ_s is the quantum yield of the sample, Φ_r is the quantum yield of the reference, n_s is the refractive index of the sample, n_r is the refractive index of the reference, A_s and A_r are the absorbances of the sample and the reference at the wavelength of excitation (500 nm), and the I_s and I_r are the integrated areas of emission bands of the sample and the reference from 600 to 900 nm, which were recorded by a red photomultiplier tube (PMT) detector. Thermal properties were characterized using thermogravimetric (TG) analyses on a NETZSCH TG 209 instrument under flowing nitrogen at a heating rate of 10 °C/min.

Synthesis of the ligand Hiqbt (1-(benzo[*b*]-thiophen-2-yl)-isoquinoline)

The C^N main ligand **Hiqbt** was synthesized from the improved Suzuki coupling reaction[2] of 2-Cl-isoquinoline while not 2-Br-isoquinoline with benzo[*b*]thien-2-y boronic acid. A mixture of 2-Cl-isoquinoline (0.653 g, 4.0 mmol), benzo[*b*]thien-2-y boronic acid (0.713 g, 4.0 mmol) was dissolved into absolute mixed solvents of toluene-EtOH (60 mL; V/V = 2:1) under an N_2 atmosphere. Then an aqueous solution (20 mL) of Na_2CO_3 (2 M) was added, and the mixture was degassed by an N_2 flow. Anhydrous $Pd(PPh_3)_4$ (190 mg, 0.2 mmol; 5 mol%) was added to

the reaction mixture and then heated at 85 °C for 48 h. The complete consumption of reagents was monitored by TLC (Hexane/AcOEt, V/V = 9:1; R_f = 0.25). After cooling to RT, the organic phase was washed with brine and extracted with absolute CH_2Cl_2 (3×20 mL) three times. The combined organic phase was dried over anhydride Na_2SO_4, and further purified with flash-column chromatography on silica gel (Hexane/AcOEt, V/V = 9:1), affording to an off-white solid. Yield: 0.762 g, 73%. Calc. for $C_{17}H_{11}NS$: C, 78.13; H, 4.24; N, 5.36%. Found: C, 78.05; H, 4.36; N, 5.29%. ^{1}H NMR ($CDCl_3$, 400 MHz): δ(ppm) 8.65 (s, 1H, -CH=N), 8.64 (s, 1H, -Ph), 7.95 (m, 3H, -Ph), 7.87 (s, 1H, -Ph), 7.76 (s, 1H, -Th), 7.68 (m, 2H, -Ph), 7.43 (m, 2H, -Ph).

Synthesis of the dimmer intermediate $[Ir(iqbt)_2(\mu\text{-}Cl)]_2$

The chloride-bridged dimmer intermediate **$[Ir(iqbt)_2(\mu\text{-}Cl)]_2$** was synthesized according to an improved procedure[3] and used directly for the next step without further purification. To a mixed solvents of 2-ethoxyethanol and D. I. water (V/V = 3:1, 24 mL), **Hiqbt** (400 mg, 2.6 mmol) and $IrCl_3{\cdot}3H_2O$ (208 mg, 1.2 mmol) were added, and the resultant mixture was heated overnight at 110 °C under a N_2 atmosphere. After cooling to RT, a saturate aqueous solution of NaCl (25 mL) was added and the dark-brown suspension was filtered. The brown solid products were further washed with D. I. water, diethyl ether and hexane, and dried at 45 °C under vacuum to constant weight. Yield: 82%.

X-ray crystallography

Single crystals for complex **$[Ir(iqbt)_2(hpa)]$**$\cdot CH_3COOCH_2CH_3$ (**1**$\cdot CH_3COOCH_2CH_3$) of suitable dimensions were mounted onto thin glass fibers. All the intensity datas were collected on a

Bruker SMART CCD diffractometer (Mo-Kα radiation and λ = 0.71073 Å) in Φ and ω scan modes. Structures were solved by Direct methods followed by difference Fourier syntheses, and then refined by full-matrix least-squares techniques against F^2 using SHELXTL.[4] All other non-hydrogen atoms were refined with anisotropic thermal parameters. Absorption corrections were applied using SADABS.[5] All hydrogen atoms were placed in calculated positions and refined isotropically using a riding model. Crystallographic data, relevant atomic distances and bond angles for complex **1**·$CH_3COOCH_2CH_3$ are presented in Tables 1-2S, respectively. CCDC number 1855382 for complex **1**·$CH_3COOCH_2CH_3$.

Cyclic voltammetry (CV) measurement

CV measurement was performed on a computer-controlled EG&G Potentiostat/Galvanostat model 283 at RT with a conventional three-electrode cell using a an $Ag/AgNO_3$ (0.1 M) reference electrode, Pt carbon working electrode of 2 mm in diameter, and a platinum wire counter electrode. CV of the sample was performed in nitrogen-saturated dichloromethane containing 0.1 M Bu_4NPF_6 as supporting electrolyte. The CV was measured at a scan rate of 100 mV·s^{-1}. The HOMO and the LUMO energy levels of each complexare calculated according to the following equations,[6] E_{HOMO} = -(E_{OX}^{on}+ 4.8) eV, E_{LUMO} = E_{HOMO} + E_g^{OPT} eV, and where $E_{OX}^{on}$is the recorded onset oxidation potential of the complex, and E_g^{OPT} is the energy band gap estimated from the low-energy edge of the absorption spectra from the samples. The HOMO and LUMO energy levels for the other used materials were obtained from the literatures.[7]

NIR-PLEDs' fabrication and testing

Each of the two NIR-PLEDs-I-IIwas fabricated on ITO (Indium tin oxide) coated glass substrates with a sheet resistance of 20 Ω per square. Patterned ITO coated glass substrates were washed with acetone, detergent, D. I. water and isopropanol in an ultrasonic bath. After being exposed under oxygen plasma for 20 min, PEDOT:PSS from water solution was spin-coated (at 2000 rpm) on the substrate and followed by drying in a vacuum oven at 140 °C for 20 min, giving a film of 30 nm thickness. The THF solution (20 mg/mL) of the mixture of PVK, OXD7 and complex **1** or **2** as the emitting layer was prepared under an N_2 atmosphere and spin-coated (at 4000 rpm) on the PEDOT:PSS layer with a thickness of 120 nm. The TmPyPB layer (15 nm) was thermally deposited onto the emitting layer especially for NIR-PLED-II-**1**. Finally, a thin layer (1 nm) of LiF followed by 100 nm thickness Al capping layer was deposited onto the substrate under vacuum of 5×10^{-6} Pa. Current density-voltage (J-V) characteristics were collected using a Keithley 2400 source meter equipped with a calibrated silicon photodiode. The NIR EL irradiance was measured through a calibrated UDT Model 280 Germanium Detector. The eternal quantum efficiencies (EQEs) of the NIR emission were obtained by measuring the irradiance in the forward direction and assuming the eternal emission profile to Lambertian.

References

1 J. H. Palmer, A. C. Durrell, Z. Gross, J. R. Winkler andH. B. Gray, *J. Am. Chem. Soc.*, 2010, 132, 9230-9231.

2 G. N. Li, Y. Zou, Y. D. Yang, J. Liang, F. Cui, T. Zheng, H. Xie and Z. G. Niu, *J. Fluoresc*, 2014, 24, 1545-1552.

3 S. Kesarkar, W. Mróz, M. Penconi, M. Pasini, S. Destri, M. Cazzaniga, D. Ceresoli, P. R. Mussini, C. Baldoli, U. Giovanella and A. Bossi, *Angew. Chem. Int. Ed.*, 2016, 55, 2714-2718.

4 G. M.Sheldrick, *SHELXL-97*, Program for Crystal Structure Refinement, University of Göttingen, Göttingen, Germany, 1997.

5 G. M. Sheldrick, *SADABS*, University of Göttingen, Göttingen, Germany, 1996.

6 H. Y. Chen, C. T. Chen and C. T. Chen, *Macromolecules,* 2010, 43, 3613-3623.

7 E. Zysman-Colman, S. S. Ghosh, G. Xie, S. Varghese, M. Chowdhury, N. Sharma, D. B. Cordes, A. M. Z. Slawin and I. D. W. Samuel, *ACS Appl. Mater. & Interfaces,* 2016, 8, 9247-9253.

Table 1S Crystal data and structure refinement for complex **1**·$CH_3COOCH_2CH_3$

Compound	**1**·$CH_3COOCH_2CH_3$
Empirical formula	$C_{44}H_{32}N_3O_5S_2Ir$
Formula weight	939.05
Crystal system	Monoclinic
Space group	*P2(1)/n*
a/Å	10.767(2)
b/Å	27.035(5)
c/Å	12.935(3)
α/°	90
β/°	99.48(3)
γ/°	90
V/Å^3	3713.9(13)
Z	4
ρ/g·cm^{-3}	1.678
Crystal size/mm	0.22 × 0.20 × 0.16
μ(Mo-Kα)/mm^{-1}	3.760
Data/restraints/parameters	7725/0/496
Quality-of-fit indicator	1.099
No. unique reflections	7725
No. observed reflections	29379
Final *R* indices [$I > 2\sigma(I)$]	R_1 = 0.0369
	wR_2 = 0.0553
R indices (all data)	R_1 = 0.0774
	wR_2 = 0.0831

Table 2S. Relevant atomic distances (Å) and bond angles (°) for complex **1**·$CH_3COOCH_2CH_3$

Compound	**1**·$CH_3COOCH_2CH_3$		
Ir(1)-C(1)	2.006(5)	Ir(1)-C(18)	2.016(5)
Ir(1)-N(1)	2.029(4)	Ir(1)-N(2)	2.155(4)
Ir(1)-N(3)	2.112(4)	Ir(1)-O(1)	2.066(3)
O(3)-H(3)···O(2)	2.568(6)		
C(1)-Ir(1)-C(18)	100.4(2)	C(1)-Ir(1)-N(1)	79.66(19)
C(1)-Ir(1)-N(2)	178.61(18)	C(1)-Ir(1)-N(3)	88.97(18)
C(1)-Ir(1)-O(1)	93.42(16)	O(3)-H(3)···O(2)	147.2(3)

Figure 1S. The ^{1}H NMR spectra for the complexes **[Ir(iqbt)$_2$(hpa)]** (**1**) and **[Ir(iqbt)$_2$(BF$_2$-hpa)]** (**2**) in $CDCl_3$ at RT.

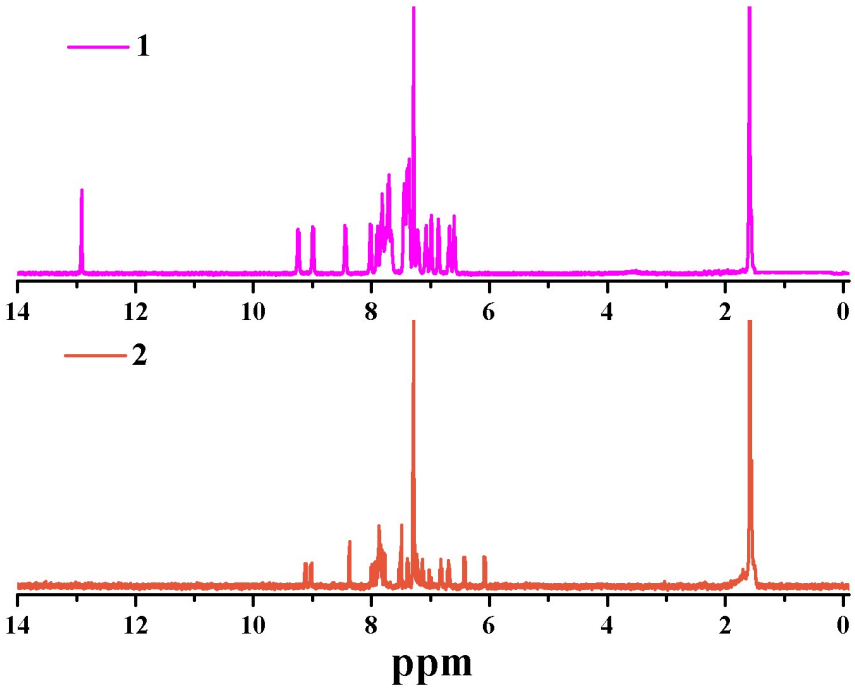

Figure 2S. TGA curves for complexes **[Ir(iqbt)$_2$(hpa)]** (**1**) and **[Ir(iqbt)$_2$(BF$_2$-hpa)]** (**2**).

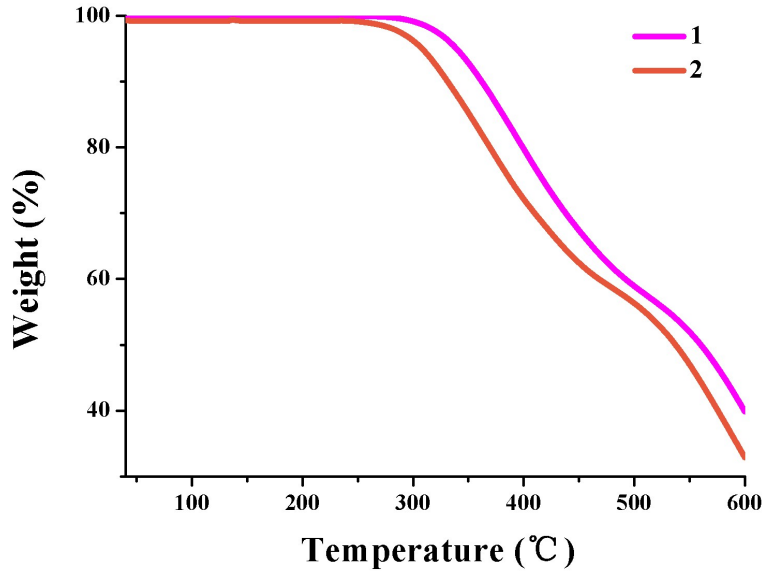

Figure 3S. UV-Visible absorption spectra (NIR absorption of complexes **1**-**2**, inset) of the ligands **Hiqbt**, **Hhpa** and **BF_2-hpa** and their Ir(III)-complexes **1**-**2** in degassed CH_2Cl_2 solution (2×10^{-5} M) at RT.

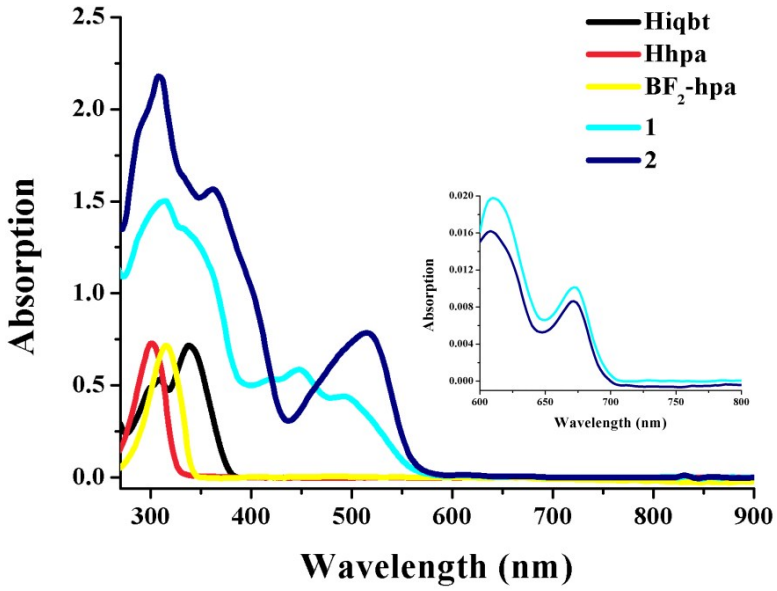

Figure 4S. Excitation spectra of the Ir(III)-complexes **1**-**2** in degassed CH_2Cl_2 solution (2×10^{-5} M) at RT.

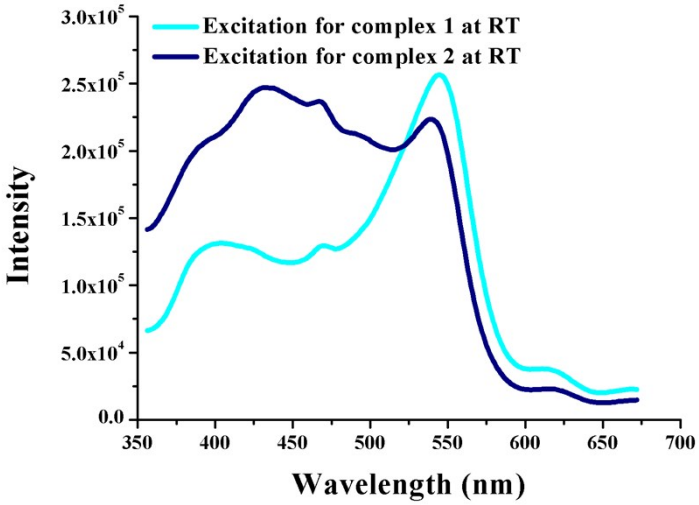

Figure 5S. Emission spectra of the ligands **Hhpa** and **BF_2-hpa** in degassed CH_2Cl_2 solution (2×10^{-5} M) at RT and their Ir(III)-complexes **1**-**2** in degassed CH_2Cl_2 solution (2×10^{-5} M) at 77 K.